Continued Table 1

Material	Lattice space group	Molecular group	RS frequency ν_v, cm^{-1}	RS linewidth $\Delta\nu$, cm^{-1}	Integral cross section, rel. units	Peak intensity, rel. units	Scattering and excitation geometry	
							K	**E**
			Mescellaneous					
NH_4SO_4 ***	—	$[SO_4]$	976.5	3.5	—	—	—	—
$Ba_3(B_3O_6)_2$	C_{3v}^6	$[B_3O_6]$	636	4.5	1	0.6	$\parallel C_3$	$\perp C_3$
SiO_2	D_3^6	$[SiO_4]$	464	7	2.2	1.2	$\perp C_3$	$\parallel C_3$

* Polycrystalline sample.

** Inhomogeneously split line.

*** Unoriented crystal.

References

1. Raman C V, Krishnan K S *Nature* (London) **121** 501 (1928)
2. Landsberg G S, Mandel'shtam L I *Zh. Rus. Fiz. Khim. Obshch.* **60** 335 (1928)
3. Placzek G *Rayleigh-Streung und Raman Effect* (Rayleigh Scattering and the Raman Effect) (Handbuch der Radiologie, 2 Auflage, Vol. 6, Pt. 2) (Leipzig, 1934) [Translated into Russian (Khar'kov: Gostekhizdat Ukr., 1935)]
4. Woodbury E J, Ng W K *Proc. IRE* **50** 2367 (1962)
5. Hellwarth R W *Phys. Rev.* **130** 1850 (1963)
6. Zubov V A, Sushchinskiĭ M M, Shuvalov I K *Usp. Fiz. Nauk* **83** 197 (1964) [*Sov. Phys. Usp.* **7** 419 (1964)]
7. Erckhart G *IEEE J. Quantum Electron.* **2** 1 (1966)
8. Bloembergen N *Am. J. Phys.* **35** 989 (1967) [*Usp. Fiz. Nauk* **97** 307 (1969)]
9. Loudon R *Adv. Phys.* **13** 423 (1967)
10. Lugovoĭ V N *Vvedenie v Teoriyu Vynuzhdennogo Kombinatsionnogo Rasseyaniya* (Introduction to the Theory of Stimulated Raman Scattering) (Moscow: Nauka, 1968)
11. Kaiser W, Maier M, in *Laser Handbook* Vol. 11 (Eds F T Arecchi, E O Shultz-Dubois) (Amsterdam: North-Holland, 1972) p. 1077
12. Grasyuk A Z *Kvantovaya Elektron.* (Moscow) **3** 485 (1974)
13. D'yakov Yu E, Nikitin S Yu *Kvantovaya Elektron.* (Moscow) **14** (10) 1925 (1987)
14. Basiev T T, Powell R C *Opt. Mater.* **11** 301 (1999)
15. Zverev P G, Basiev T T, Prokhorov A M *Opt. Mater.* **11** 335 (1999)
16. Belevtseva L I et al. *Opt. Mekh. Promst.* **56** (4) 38 (1989)
17. Zverev P G et al. *Opt. Mater.* **11** 315 (1999)
18. Verenberg V A, Karpukhin S N, Mochalov I V *Kvantovaya Elektron.* (Moscow) **14** 1849 (1987) [*Sov. J. Quantum Electron.* **17** 1178 (1987)]
19. Mochalov I V *Opt. Zh.* (11) 4 (1995)
20. Eremenko A S, Karpukhin S N, Stepanov A I *Kvantovaya Elektron.* (Moscow) **7** 196 (1980) [*Sov. J. Quantum Electron.* **10** 113 (1980)]
21. Zverev P G et al. *Opt. Commun.* **97** 59 (1993)
22. He Ch., Chyba T H *Opt. Commun.* **135** 273 (1997)
23. Karpukhin S N, Yashin V E *Kvantovaya Elektron.* (Moscow) **10** 1992 (1984) [*Sov. J. Quantum Electron.* **14** 1337 (1984)]
24. Voĭtsekhovskiĭ V N, Karpukhin S N, Yakobson V E *Opt. Zh.* (11) 30 (1995)
25. Basiev T T et al. *Izv. Akad. Nauk SSSR, Ser. Fiz.* **46** 1600 (1982)
26. Basiev T T, Osiko V V, Mirov S B *IEEE J. Quantum Electron.* **QE-24** 1052 (1988)
27. Basiev T T, Mirov S B, in *Room Temperature Tunable Color Center Lasers* (Laser Science and Technology Books Series, 16) (Chur, Switzerland: Harwood Academic Publishers, 1994) p. 1
28. Basiev T T et al. *Kvantovaya Elektron.* (Moscow) **14** 2452 (1987) [*Sov. J. Quantum Electron.* **17** 1560 (1987)]
29. Basiev T T et al. *Izv. Akad. Nauk SSSR, Ser. Fiz.* **54** 1450 (1990)
30. Zverev P G, Basiev T T, in *Proc. All-Union Conference 'Optika Laserov'* Vol. 2 (Leningrad, 1993) p. 363
31. Zverev P G, Basiev T T *J. Phys. IV* (Paris) **4** C4-599 (1994)
32. Zverev P G, Basiev T T, Prokhorov A M, in *CLEO/Europe'94* (Tech. Digest 94TH0614-8, 1994) p. 154
33. Zverev P G et al., in *Laser Methods of Surface Treatment and Modification* (Proc. SPIE, Vol. 2498) (Bellingham: SPIE, 1994) p. 164
34. Basiev T T et al., in *CLEO/Europe'94* (Tech. Digest 94TH0614-8, 1994) p.125
35. Basiev T T et al., in *Laser Methods of Surface Treatment and Modification* (Proc. SPIE, Vol. 2498) (Bellingham: SPIE, 1994) p. 171
36. Zverev P G, Basiev T T, in *OSA Proceedings on Advanced Solid State Lasers* Vol. 24 (Eds B H T Chai, S A Pain) (Washington, DC: OSA, 1995) p. 288
37. Zverev P G et al., in *Advanced Solid State Lasers* Vol. 1 (Eds S A Pain, C Pollok) (Washington, DC: OSA TOPS, 1996) p.554
38. Murray J T et al. *Opt. Mater.* **11** 373 (1999)
39. Basiev T T et al. *Pis'ma Zh. Eksp. Teor. Fiz.* **37** 192 (1983) [*JETP Lett.* **37** 229 (1983)]
40. Zverev P G, Basiev T T *Kvantovaya Elektron.* (Moscow) **22** 1241 (1995)
41. Zverev P G et al. *Opt. Lett.* **20** 2378 (1995)
42. Basiev T T et al., in *Advanced Solid State Lasers* Vol. 19 (Eds W R Rosenberg, M M Fejer) (Washington, DC: OSA TOPS, 1998) p. 546
43. Basiev T T et al. *Appl. Opt.* **38** 594 (1999)
44. Basiev T T et al. *Opt. Mater.* **11** 307 (1999)
45. Basiev T T et al., in *Proc. Laser '98 Conference, Tucson, Dec. 1998* (Eds V J Corcoran, T A Goldman) (McLean, VA: STS Press, 1999) p. 712
46. Basiev T T et al., in *Tech. Digest: Novel Lasers and Devices — Basic Aspects* (CLEO-Europe Focus Meeting '99, Munich, 1999) p. 160

PACS numbers: **42.62.–b**, 61.80.Ba

Application of laser-driven shock waves in studies of thermal and mechanical material properties

I K Krasyuk

Lasers furnish a unique opportunity to study the physical properties of a material at high energy density [1]. As revealed by laser fusion research, for instance, at the center of spherical shell targets exposed to pulse laser radiation it is possible to attain a significant compression of the target material (1000 g cm^{-3}) and to heat it to high temperatures (100 keV).

Under typical conditions, a high-temperature plasma forms at the target surface under laser pulse irradiation. The hydrodynamic plasma expansion is responsible for the

ablation pressure acting on the target due to the recoil momentum. As a result, a shock wave is formed in the target, which can range up to hundreds of megabars in amplitude. Behind the shock front, there occurs heating and compression of the target material.

The experimental techniques developed to date enable laser-produced shocks to be used in studies of the thermodynamic and mechanical characteristics of materials in extreme conditions. One important application of laser-produced shocks is the construction of wide-range semiempirical equations of state of a substance. In this case, the possibility appears to probe the previously unexplored domains of phase diagrams.

The investigative technique rests on the use of algebraic relationships between the hydrodynamic quantities at the jump (shock-wave) surface, which follow from the general laws of conservation of mass, momentum, and pressure [2]:

$$P = P_0 + U\frac{D}{V_0}\,,$$
$$V = (D - U)\frac{V_0}{D}\,,$$
$$E = E_0 + 0.5(P_0 + P)(V_0 - V)\,. \qquad (1)$$

Here, V is the specific volume, P is the pressure, E is the internal energy, D is the velocity of the shock-wave surface in an unperturbed material, U is the mass velocity, i.e. the velocity of particles behind the shock, and the subscript '0' refers to the quantities which characterize the unperturbed material in front of the shock wave.

By recording any two of the five parameters P, V, D, U, and E, with the use of relationships (1) it is possible to find the hydrodynamic and thermodynamic characteristics of a substance and establish the relation between them employing the caloric equation of state

$$E = E(P, V)\,. \qquad (2)$$

For metals, the kinematic parameters D and U are usually measured. The measurements reduce to recording the time a shock-wave surface takes to propagate a fixed (reference) distance. In the cases of practical significance, the accuracy of measuring the phase D and group U velocities of motion of the shock should not be worse than 5–10%.

Using dynamic diagnostic techniques which rest on relationships (1), to obtain the shock adiabatic curve implies that the hydrodynamic flow of the material under study is stationary and unidimensional. The unidimensional and stationary state is afforded by choosing the target thickness and the diameter of the irradiation spot. The initial state of the target is of significance too, because the generation of shock waves by lasers is associated with the formation of a high-temperature plasma at the front surface of the target, which can result in the preheating of the target material by the X-ray radiation of the plasma corona and by the stream of fast electrons.

The availability of the equation of state in the caloric form (2) makes it possible to conduct hydrodynamic calculations of adiabatic material flows. However, taking into account the processes involving heat transfer and radiation calls for explicit assignment of the temperature as a function of the pressure and the volume:

$$T = T(P, V)\,. \qquad (3)$$

For metals, measuring the temperature of a material behind the shock by optical techniques is an intricate task primarily due to the screening of the radiation from hot plasma regions by the material vapor in the rarefaction wave. Notice that owing to experimental difficulties and the ambiguity of interpretation of the resultant data, only a small number of available papers on the laser generation of shock waves are dedicated to direct temperature measurements of the material behind the shock in metals.

Because the laser action is short in duration, the experimental study of thermodynamic material properties, employing laser-produced shock waves, is a challenge. It is essential that the design and the accuracy of target fabrication, the quality and the power of the laser beam, the spatial and the time resolution of the recording equipment should meet several requirements.

For a typical duration of laser irradiation of about 1 ns, the target thickness should not exceed 15–20 μm, while the diameter of the irradiation spot should be no less than 150–200 μm. The difficulties emerging in this case can be overcome by resorting to measuring equipment with a high time and spatial resolution and by using targets made of the material under study in accordance with stringent requirements on accuracy and purity.

Another line involving the use of laser-produced shock waves is the study of mechanical properties of a material deformed at an ultrahigh rate. When a shock wave reflects at the target rear surface, a region of tensile stress ('negative' pressures) appears nearby. As a consequence, spalling effects develop at the rear side of the target, which result in the detachment of a target fragment.

The use of laser-produced shock waves permits the spalling effects to be studied at deformation rates that exceed those previously attained by nearly two orders of magnitude. In this case, the attainment of the theoretical ultimate strength proves to be quite realistic. In studies of the spalling effects, one of the essential features required of the processes occurring is that they be unidimensional.

Experiments on the laser generation of shock waves were staged on high-power Nd-glass laser facilities at the Center for Community Use in the Institute of General Physics, Russian Academy of Sciences; the Center functions under the auspices of the Russian Foundation for Basic Research. Use was made of the fundamental radiation with a wavelength of 1.06 μm as well as of its second harmonic. The possibility existed to perform experiments with laser irradiation ranging from 2.5 to 80 ns in duration and a controllable pulse shape.

The intensity of laser radiation at the target could be as high as 4×10^{14} W cm^{-2} and the corresponding ablation pressure as high as 50 Mbar. The recording complex comprised high-speed electronic and optical measuring instruments. For the first time, fiber light guides and optical components around them were used in the diagnostics of strong shock waves. A laser interference velocity meter of specific design was employed to study the spalling effects.

A package of numerical codes was elaborated to model the phenomena under investigation, starting from hydrodynamic equations which incorporate thermodynamically complete wide-range semiempirical real equations of state of the materials under study. In the calculation of the coefficients of light absorption in the rarefaction wave, a numerical code was employed which rested on the application of a generalized 'chemical' model including the effects of nonideality, degen-

eracy, and the metal – nonmetal transition. As a simpler way of calculating the light absorption coefficients, the Kramers – Unsold formula appropriate in the case of a gas comprised of hydrogen-like atoms was also used.

A more comprehensive description of the experimental and numerical techniques for studying the phenomena associated with laser-driven shock waves can be found in Ref. [3].

One of the latest achievements in studies of thermal material properties consists in the measurement of the temperature of the material behind the shock-wave surface in an aluminium target and the study of its preheating [4]. This work was conducted in the context of international cooperation. The experiments were carried out at the laser facility of LULI (Ecole Polytechnique, Palaiseau, France).

The laser radiation with a wavelength of 0.53 μm was 0.6 ns in duration. The intensity of laser radiation at the target run as high as 3×10^{13} W cm^{-2}. In experiments, use was made of step-like aluminium targets with a 9.4-μm thick base, a 4-μm high step, and a transition zone approximately 2 μm in width. The pressure behind the shock was determined by the known shock adiabatic curve of aluminium, from the measured time it took for the shock wave to propagate the reference distance, viz. the target step height. A two-channel pyrometer with a time resolution of ±5 ps was used to measure the 'color' temperature of the material in the rarefaction wave.

The results of one of the experiments are given in Fig. 1. The pressure measured behind the shock-wave surface was 6.8 Mbar. The time variation of the measured 'color' temperature of the material in the rarefaction wave is shown by a bold solid line. A thin solid line represents the calculated maximum values of the real temperature of the material in the rarefaction wave. It is evident that the measured and calculated temperature profiles coincide within the limits of experimental error.

The dotted and the dashed lines in Fig. 1 show the radiation 'color' temperatures at the target rear surface, calculated respectively by the dedicated numerical code and the Kramers – Unsold formula. It was determined that the lengthening of the wave front in the experimental curve is indicative of the preheating of the target material in front of the shock wave. Presented at the top of Fig. 1 are the layout of experiment on the laser generation of shock waves and one of the photochronograms of the emission originating when the shock front reaches the free surface of the step-like target.

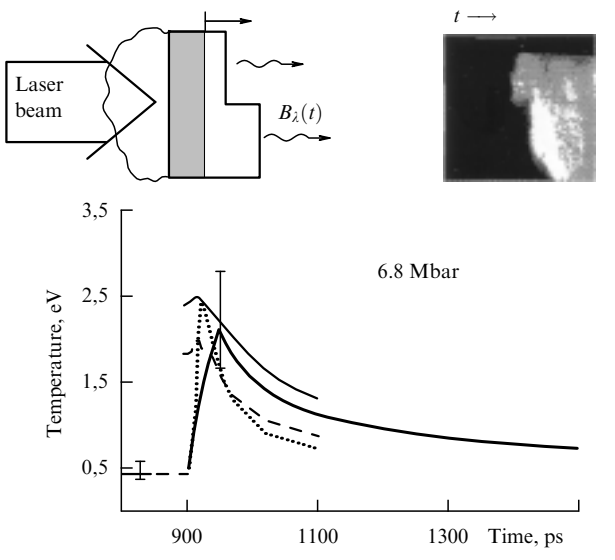

Figure 1. Thermal properties of shock-compressed aluminium.

One interesting outcome of the study of spalling effects is the measurement of the spalling strength of the AMg6M aluminium alloy in relation to the deformation rate [5]. The mechanical strength was found to tend to the theoretical ultimate strength as the deformation rate approaches 10^8 s^{-1}. The collection of experimental data encompassing both explosion and laser experiments is shown in Fig. 2. Given at the top left in Fig. 2 is a photograph of the rear side of the target subsequent to laser irradiation. The breakaway material layer nearly detached from the target is clearly visible.

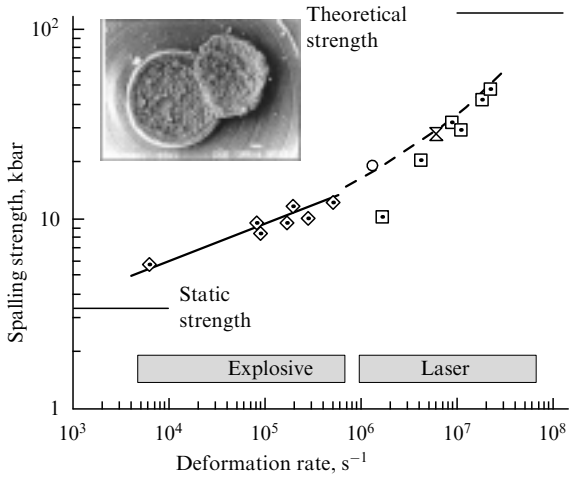

Figure 2. Spalling strength of the AMg6M aluminium alloy.

The studies performed in cooperation between the staff members of the Institute of General Physics of the Russian Academy of Sciences (RAS), the Scientific Research Center for Thermal Physics of Pulse Exposures at the Joint Institute for High Temperatures (RAS), the Institute of Energy Problems in Chemical Physics (RAS), the Physics Department of the University of Milan (Milan, Italy), and LULI (Ecole Polytechnique, Palaiseau, France) show that lasers are a promising tool for the generation of shock waves for the purpose of studying the thermal and mechanical properties of materials subjected to extreme conditions. The present difficulties can be circumvented in the near future.

This work was supported by the Russian Foundation for Basic Research (grants Nos 94-02-03413 and 97-02-16456) and INTAS–RFBR (project No. 95-0631).

References

1. Anisimov S I, Prokhorov A M, Fortov V E *Usp. Fiz. Nauk* **142** 395 (1984) [*Sov. Phys. Usp.* **27** 181 (1984)]
2. Zel'dovich Ya B, Raĭzer Yu P *Fizika Udarnykh Voln i Vysokotemperaturnykh Gidrodinamicheskikh Yavleniĭ* (Physics of Shock Waves and High-Temperature Hydrodynamic Phenomena) (Moscow: Nauka, 1966) [Translated into English (New York: Academic Press, 1966 – 1967)]
3. Vovchenko V I, Krasyuk I K, Semenov A Yu, in *Physical Processes in Conic Shell Targets* (Proceedings of the Institute of General

Physics, Russian Academy of Sciences, Vol. 36) (Moscow: Nauka, 1992) p. 129
4. Batani D et al. *Control Fusion* **41** 93 (1999)
5. Vovchenko V I et al., in *Laser Interaction and Related Plasma Phenomena* Vol. 1 (Eds S Nakai, G H Miley) (New York: AIP Press, 1995) p. 369

PACS numbers: **62.50.+p**, 62.20.Dc, 64.70.Kb, 64.70.Pf

Transformations in amorphous solids under high pressures

A G Lyapin, V V Brazhkin, E L Gromnitskaya, O V Stal'gorova, O B Tsiok

Phase polymorphism at high pressure has been much studied for many crystalline solids [1]. With an increase in pressure, in crystals there occur phase transitions (primarily of the first order) to a closer packing of atoms in accordance with the Le Chatelier principle. Recently, indications have emerged that the first-order phase transitions are possible in many melts too, even though these transitions can supposedly be realized only in the supercooled liquid domain, well below the melting temperature [2, 3].

In a series of papers, most often using water as an example, a parallel is drawn between the phase transitions in a supercooled liquid and the transformations in the corresponding amorphous solid phases [4–6]. However, analogies of this sort are not fully justified because amorphous substances are nonergodic systems and have no domain of thermodynamic stability in the phase diagram at all, whereas the notion of 'phase' itself can be applied to amorphous modifications only rather conventionally. Amorphous substances exist in the metastable state only at sufficiently low temperatures, when diffusion is frozen. At the same time, the relaxation processes in amorphous phases can proceed even at low temperatures [7].

Nevertheless, a distinct short-range (local) order does exist in amorphous and vitreous substances [7]. This brings up the natural question: are jump-like changes of the volume, the local-order structure, and of other properties in the amorphous phase possible on compression? It is well known that several tetrahedral amorphous semiconductors and chalcogenide glasses crystallize under pressure (see paper [8] and references cited therein).

At the same time, the existence of reversible transformations between amorphous modifications involving changes of the local-order structure and the density (in the subsequent discussion also referred to as structural or coordination transitions) has been firmly established by different experimental techniques for SiO_2 and GeO_2 oxide glasses and amorphous H_2O ice [9–17]. Moreover, there is experimental evidence for the structural transitions under pressure in other amorphous materials, too. The case in point are amorphous modifications of carbon [18, 19].

Most intriguing is elucidation of the mechanism of the like transformations. The phase transitions in crystals occur through nucleation and diffusive growth of the new phase (diffusive transformations) or as coherent atomic displacements in the lattice (martensite transformations). Neither of the two possibilities can be realized in the case of transformations between amorphous phases. In this connection, the question of not only the mechanism, but the very possibility of abrupt structural transitions in amorphous materials under compression has until recently remained an open question.

The results of precision measurements on the density of SiO_2 and GeO_2 oxide glasses under pressure are given below. The transformation between low- and high-density amorphous modifications (*lda* ↔ *hda*) of H_2O ice was studied by an ultrasonic technique. The study of the transformation kinetics and the dynamics of amorphous networks in the neighborhood of transition points received primary emphasis. Conceptual approaches to the description of transformations between amorphous phases are considered.

The densities of *a*-SiO_2 and *a*-GeO_2 were measured by a tensometric method in hydrostatic conditions up to 9 GPa [20]. One of the main advantages of this procedure is the high precision of measurements on absolute (about 0.3%) and relative (of the order of 10^{-3} %) volume changes alike, the latter being particularly important for studying relaxation processes. Some results of the measurements are given in Figs 1 and 2. Experimentally, *a*-GeO_2 proved to be the most convenient object, where the coordination transition was observed in the 4–13 GPa range [13–15]. Along with the investigation of the equation of state under continuous

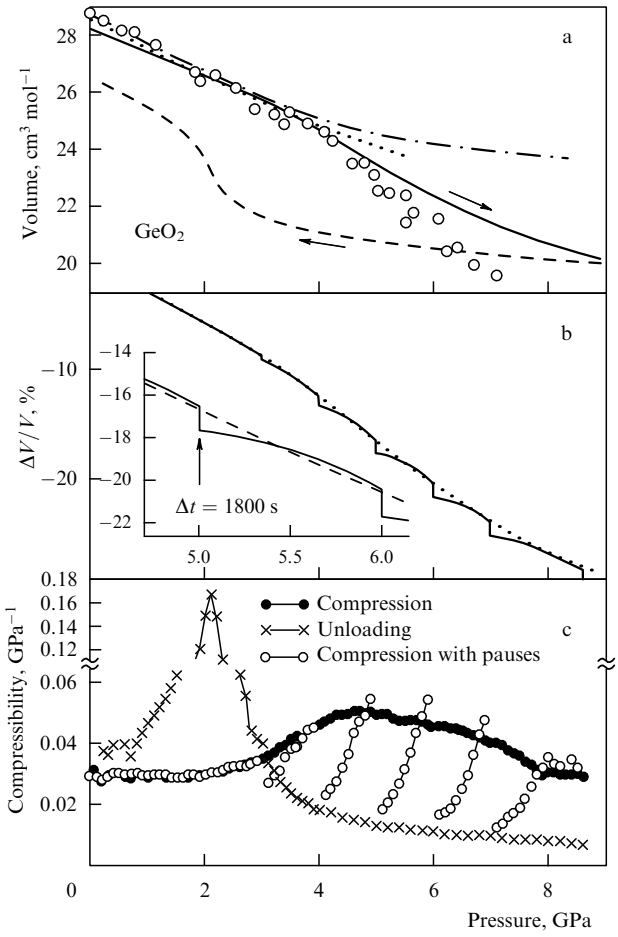

Figure 1. (a) Quasi-static equation of state of *a*-GeO_2 as compared with the data of Ref. [15] (circles) and with the equations of state obtained from ultrasonic (the dashed line) [19] and Brillouin (the dot-and-dash line) [20] experiments; (b) volume change in the experiment with a continuous variation of the pressure (the dashed line) compared with that in the experiment with a fixed pressure (the solid line); (c) change of compressibility under different experimental conditions.